Fault Distance Estimation Method for Two-Terminal Transmission Line

Dr. Ravi Gupta[1], Preet Lata[2]
[1]Assistant Professor, Engineering College Bharatpur, Rajasthan, India, raviguptabtp@gmail.com
[2] Assistant Professor, Engineering College Bharatpur, Rajasthan, India, preetklata@gmail.com

ABSTRACT

A new fault distance estimation method is proposed for unbalanced earth faults based on Initial Traveling Wavefronts (ITWs) in aerial mode and earth mode of travelling wave. The aerial and earth mode of travelling waves are calculated using phase-mode transformation theory. Thereafter, the time of Wavelet Transform Modulus Maxima (WTMM) of aerial mode component and earth mode is analyzed for fault distance estimation. This algorithm does not require synchronized measurement and pre-estimation of transmission line parameters. The efficacy of the algorithm is verified by generating diverse fault cases using PSCAD/EMTDC software. Results shown in paper shows its capability of accurate fault distance estimation under comprehensive variation in type of fault, line length, fault inception angle, fault resistance and source impedance. Subsequently, its accuracy remains almost constant considering errors in line parameters.

Key words: Two-terminal transmission line, high impedance fault, fault distance estimation, unsynchronized measurement.

1. INTRODUCTION

The repair time and reliability of power system can be improved by estimating the accurate fault distance. Various fault location methods have been reported in past by many researchers which can be broadly classified into two categories: (1) Impedance-based algorithms [1]-[8]; and (2) travelling-wave based algorithms [9]-[19]. Most of the impedance-based algorithms needs to compute phasors, synchronized measurement of voltage/currents, and/or superimposed values which causes increase in financial burden and reduces the reliability. Further, these schemes are sensitive to variation in line and source impedance parameters.

Travelling-wave-based method locates the fault by utilizing the arrival time of initial travelling wave and the travelling wave velocity. These methods often use the aerial-mode component of travelling wave obtained by phase-mode transformation. The conventional travelling-wave-based method can be classified into single-ended algorithm [9]-[11] and double-ended algorithm [12]-[16]. Above mentioned issues with impedance-based algorithms were resolved by many utilities using one-terminal traveling-wave-based methods for many years [9].

Although these single-ended algorithms provide fault location quick in time and free from limitation due to requirement of data synchronization, performance for close-in faults are problem [10-11]. The traveling-wave-based fault-location algorithms which use data from both line ends to locate the faults are less susceptible to errors than one-terminal methods [12]. However, double-ended algorithms require the data from both line ends which is also to be synchronized, which is often reported as a drawback that can jeopardize the accuracy of two- and multiterminal traveling wave-based FLs [12-16].

Global Positioning System (GPS) is most often to use with data-acquisition system (DAQ) to provide solution for common time reference for power system protection devices [17]. This arrangement provides the time-stamping of data with an accuracy better than ± 1 μs [18], [19]. It equivalents, for 60-Hz power systems, to local and remote data synchronism errors of about $\pm 0.0216°$, which yield the traveling-wave-based algorithms for the fault-location errors of the order of 300 m only [19]. However, in reality, several other synchronization problems still exist. It is also to be noted that every substation is not necessarily be installed with common time reference sources. Hence, the possibility of the loss of the time reference signal has been extensively reported. Also, single as well as double-ended algorithms are also inherently sensitive to inaccuracies in pre-estimated transmission line parameters like other impedance-based algorithms. It is because of utilization of line parameters to calculate the propagation velocity which affects the accuracy of algorithm greatly. Hence, the application of two-terminal

traveling wave-based fault-location methods has been limited.

Earth faults occur in transmission lines generates travelling wave includes not only the aerial mode but also earth mode component. This paper proposed a novel fault location algorithm for unbalanced earth faults based on the propagation time delay between aerial and earth mode component of travelling wave. This algorithm does not require any synchronized measurement, pre-calculation of line parameters and wave velocity. Various test results obtained for diverse cases reveal that the proposed method is robust and accurate against wide variation in fault parameters, errors in line parameters and noise in the measured signals.

2. BASIC PRINCIPLE OF PROPOSED ALGORITHM

2.1 Initial travelling wave and phase-mode transformation

Current signals propagating in transmission lines are in the forms of electromagnetic waves. These waves can be expressed as

$$I(x,w,t) = \sqrt{2}I^+ e^{-\alpha(w)x} \cos(wt - \beta(w)x + \phi^+)$$
$$+ \sqrt{2}I^- e^{-\alpha(w)x} \cos(wt - \beta(w)x + \phi^-) \quad (1)$$

where $a(w)$ and $\beta(w)$ are defined as the attenuation factors and phase distortion factors of line, respectively. Equation (1) shows that a traveling wave consists of a forward wave and a backward wave. The traveling wave attenuates exponentially with distance. The propagation coefficient ($\gamma = a + j\beta$) plays an important role in the propagation of the traveling wave.

In order to decouple the complex electromagnetic coupling relationship exists in the three-phase transmission lines, phase-mode transformation is usually used. This paper utilizes the aerial and earth mode of travelling wave which is calculated by transforming matrix as given below in equation (2).

$$\begin{bmatrix} U_0 \\ U_1 \\ U_2 \end{bmatrix} = \frac{1}{3} \begin{bmatrix} 1 & 1 & 1 \\ 1 & -1 & 1 \\ 1 & 0 & -1 \end{bmatrix} \begin{bmatrix} U_A \\ U_B \\ U_C \end{bmatrix} \quad (2)$$

2.2 Wavelet modulus maxima

The high frequency travelling waves are nothing but the superimposed components hidden in the post fault signals. It can be extracted and localized well in frequency and time domain The modulus maxima of Discrete wavelet transform (DWT) has advantage of reliable detection of discontinuity such as of travelling waves due to its dyadic nature. Wavelet transform divide the signal in different frequency band corresponding to each scale [20]. However, provided that the signal is sampled down by a factor 2 in each dimension, DWT's real-time application for fault

analysis is hardly affected. For example, when applying WT to current multi-line signals, it is crucial that the wavelet coefficients remain time-invariant for each other. A time-invariant wavelet transformation is thus more suitable for the study of faults. The Maximum Overlap Discrete Wavelet Transform (MODWT) is a similar version of DWT except that it retains all the samples in every scale unlike DWT uses sampling down by 2. This allows for high frequency analyzes in real time with faster computations [20, 21]. In the present work, therefore, MODWT has been used to measure the cumulative wavelet transform modulus (WTMM).

The current signal wavelet coefficients (w) of the jth scale i_x at t^{th} tth sample can be expressed as:

$$w_j(t) = \sum_{l=1}^{L_j} \tilde{h}_j(l) i_x(t - L_j + l) \quad (3)$$

Where, $\tilde{h}_j(l)$ are rescaled coefficients of low and high pass filter at j^{th} scale. L_j is number of filter coefficients at j^{th} scale.

$$L_j (2^j - 1)(L-1) + 1 \quad (4)$$

Where, L is the number of mother wavelet Filter Coefficients.

At a given scale, WTMM is classified as local maxima or minimum.

$$WTMM_j(t) = \begin{cases} w_j(t), & \text{if } \Delta w_j(t) > 0 \, \& \, w_j(t+1) \\ 0, & \text{otherwise} \end{cases} \quad (5)$$

Where, $\Delta w_j(t) \; (= |w_j(t)| - |w_j(t-1)|)$ is difference in between wavelet coefficients.

The selection of proper mother wavelet is very important for effective application of wavelet transform. The prior knowledge of application and signal to be analyzed may help in proper selection of mother wavelet. Important aspects to consider when selecting the mother wavelet: a) pictorial resemblance to the original signal b) number of fading moments present c) computational burden, and d) filter characteristics. Many past publication has claimed that the best results are obtained with the mother wavelets having closest visual similarity to original signal. As dicussed, the high frequency travelling waves are nothing but the superimposed components hidden in the post fault signals. Hence, the first order step functions can be used to describe the current TWs. The Current Transformers (CTs) connected to the axes, however, operate as a linear second-order mechanism that triggers the damped oscillations at the initial wavefront instant of arrival. WTMM provide way to

correctly represent the initial wavefront arrival instant, as the polarity and steep of initial wavefronts remain unchanged [22]. Despite this, visual inspection of various mother wavelets may lead to the conclusion that Db1 (Haar) is the closest representation of a step signal (TW). It is worth noting that the mother wavelet should have at least n − 1 vanishing moments in order to detect a discontinuity of the order-n. Therefore the mother wavelet should have at least one vanishing moments in order to detect the initial TWs at the secondary CT. This also means a minimum requirement for computations. To compare the capacity of different mother wavelets to extract WTMMs, scale-1 wavelet coefficients are displayed corresponding to different mother wavelets, such as Symlets (Sym), Daubechies (Db), and Coiflets (Coif), with limited vanishing moments. In Figure, TW induced by fault initiation and corresponding scale-1 wavelet coefficients are shown for the above mentioned mother wavelets. It can be observed that Daubechies (Db) closely resembles the sudden transition, like TWs, out of all the wavelets.
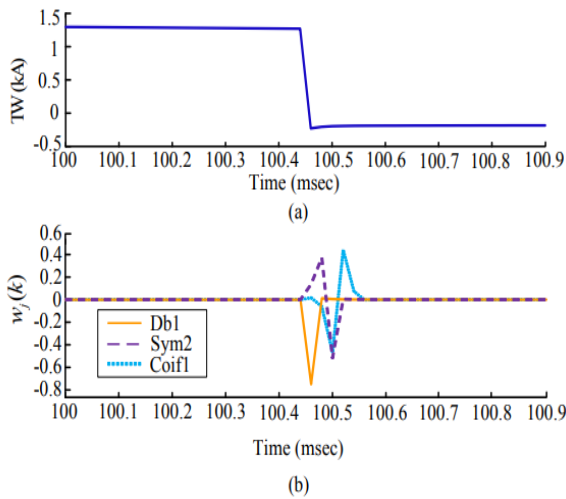

Figure 1: Scale 1 wavelet coefficient for different mother wavelet

The noise signal and travelling wave signal is similar in nature. Both has the singularity. Thus, signal should be denoised before wave front detection. This paper utilized the wavelet transform for multi-scale singularity detection [21]. Hence, the de-noising the traveling wave signal can be realized with different inherent performance characteristics of traveling wave and noise on different scales as shown in Fig. 2. It can be observed form Fig. 2 that the noise has different impact on different scale. Signal at the scale 1 completely submerges travelling wave signal. At the same time, its maximum value at scale 2 down to less than one-fourth of the initial amplitude of traveling wave. Further, the

noise level at scale 3 is very weak. It can be concluded that the high scale wavelet transform attenuates the noise effectively and the value of its modulus maxima increases. Hence, high scale wavelet transform makes it easy to detect wave front even with high noise content in signal.
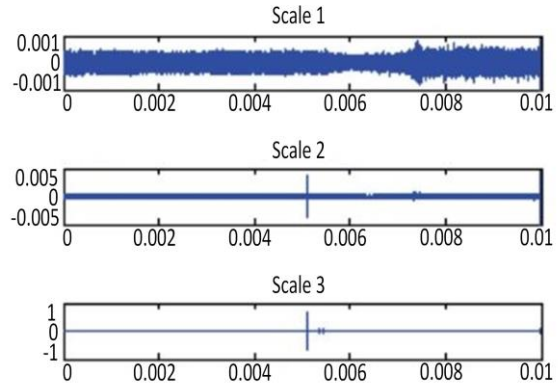

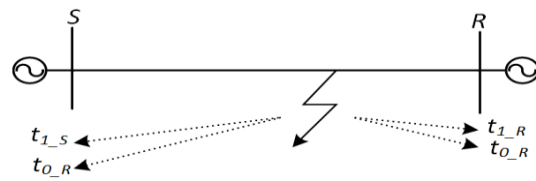**Figure 2:** Aerial and earth mode travelling wave propagation along line

Figure 3: Single line diagram of simulated two-terminal transmission line

2.3 Proposed fault location algorithm

The wavelet transform is performed over aerial mode and earth mode, respectively, and the time corresponding to their first respective modulus maxima are the arrival time for the initial wave head of aerial mode and earth mode. From this, the mode transmission time delays of the two can be obtained as in equation (2) and (3).

It is also to be noted that the attenuation of earth mode component increases as the fault distance increases and propagation velocity decreases. Whereas, the propagation velocity for aerial component remains almost constant.

$$v_1 = x / t_{1\_S} \text{ and } v_0 = x / t_{0\_S} \qquad (6)$$

$$v_1 = (l - x) / t_{1\_R} \text{ and } v_0 = (l - x) / t_{0\_R} \qquad (7)$$

Time difference of wave arrival (TDWA) for both the terminal S and R can be written as equation (8) using equations (6) and (7).

$$\left. \begin{array}{l} t_{0\_S} - t_{1\_S} = x(v_0 - v_1) / v_0 v_1 \\ t_{0\_R} - t_{1\_R} = (l - x)(v_0 - v_1) / v_0 v_1 \end{array} \right\} \qquad (8)$$

The TDWA data is transferred by PMU, connected at both

terminals of transmission line, to central station. Then, the expression of fault location can be written as equation (9).

$$x = l(t_{0\_S} - t_{1\_S}) / (t_{0\_S} - t_{1\_S} + t_{0\_R} - t_{1\_R}) \qquad (9)$$

It can be observed from the equation (9) that the expression of fault distance requires no propagation velocity information. It also analyzes the arrival time difference of wave for aerial and earth mode. Hence, the proposed algorithm is independent of data synchronization and line parameters. It is to be noted that this paper does not consider the communication errors associated with streaming of individual PMU data.

3. PERFORMANCE EVALUATION

PSCAD/EMTDC is used to model a 230 kV two-terminal transmission line as shown in Fig. 3. A Large numbers of simulation cases with varying system parameters and faults are generated.In all test cases, a sampling frequency of 2 MHz is used. The percentage fault distance estimation error is calculated as per (10).

$$\text{Error (\%)} = \frac{|\text{estimated location-actual location}|}{\text{length between terminal S and R}} \times 100 \qquad (10)$$

3.1 General fault

A line-ground (LG) fault with fault resistance of 10 Ω and 10° fault inception angle was simulated at 10 km from terminal S. The WTMM coefficients of aerial and earth mode signal of current at terminal S and R are shown in Fig. 4 (a) and Fig. 4 (b), respectively. As shown in Fig. 4 (a), the value of t_{0_S} and t_{1_S} for terminal R is 0.100044 and 0.100037 seconds, respectively, for which TDWA is 7 μseconds. Similarly, TDWA for terminal R is 72 μseconds. The value of fault distance is calculated using the expression given in equation (8) with values of TDWA of terminal S and R. It gives the fault distance value of 9.721 km from terminal S. The percentage error for this fault condition is around 0.279.
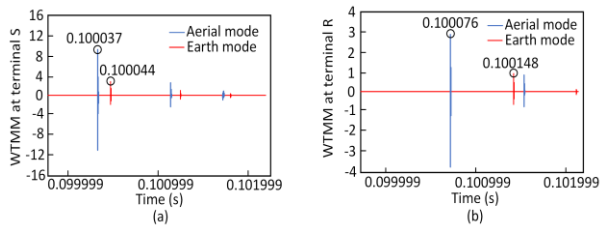

Figure 4: Result of proposed algorithm in terms of arrival time for a ground fault at 10 km from terminal S

3.2 Influence of varying fault distance and fault resistance

The performance of proposed scheme is verified for different fault locations by simulating the line-ground fault from 10 km to 90 km from terminal S. The results of proposed algorithm in terms of TDWA and fault distance estimation error are given in Table I. It can be observed from Table I that the maximum percentage error in fault distance estimation is 0.94 for fault at 70 km from terminal S.

Table 1 Results of proposed algorithm for different fault locations

TDWA (μsecond)		Fault distance (from terminal S)		
Terminal S	Terminal R	Actual (km)	Estimated (km)	Error (%)
7	72	10	9.72	0.28
12	49	20	19.73	0.27
18	41.5	30	30.25	0.25
24.5	37.5	40	39.51	0.49
29.5	31.5	50	49.16	0.84
37.5	24.5	60	60.48	0.48
41.5	17	70	70.94	0.94
47.5	12.5	80	79.16	0.84
72	7	90	90.78	0.78

Fault resistance shown negative impact on many fault location algorithms. In order to investigate the sensitivity of proposed method for fault resistance, fault condition corresponding to maximum error case in Table I is simulated with varying fault resistance from 0.1 Ω to 100 Ω. Result in terms of fault distance estimation error is shown in Fig. 5. It is observed from Fig. 5 that the fault distance estimation error increases from 0.94 to 1.12 for variation in fault resistance up to 100 Ω which is acceptable. This confirm effectiveness of the proposed algorithm for high as well as low value of fault resistance.

3.3 Impact of ground resistivity

The performance of the proposed algorithm is checked for different ground conditions. Table II shows the resistivity with different ground conditions.

Table 2 Resistivity of different Soils

Ground conditions	Resistivity (Ω-m)
Clay	50
Loess	200
Sand	1000

The results of the proposed algorithm for LG faults with varying ground conditions are shown in Table III. From the tabulated results, it can be concluded that the ground resistivity has no effect on the proposed scheme.

Table 3 Results of Proposed Algorithm for different Ground Resistivity

Resistivity (Ω-m)	Fault distance (from terminal S)		
	Actual (km)	Estimated (km)	Error (%)
50		14.71	0.29
200	15	14.73	0.27
1000		14.70	0.30
50		44.46	0.54
200	45	44.41	0.59
1000		44.38	0.62
50		95.82	0.82
200	95	95.87	0.87
1000		95.91	0.91

3.4 Effect of noise in the measurements

In actual area, the measurement data are skewed due to transducers and environmental noise. A white Gauussian noise with specific signal-to - noise ratio (SNR) of 20 , 30 and 40 dB is integrated into the measured data to reproduce the real field data. Specific fault cases were tested at various positions of the fault. The results are expressed in Fig in terms of maximum percentage error for all simulated error cases for LG faults. It can be observed from Fig. 6 that though the maximum error increases, its value remains less than 2.25 % even with worst case i.e. SNR = 20 dB.
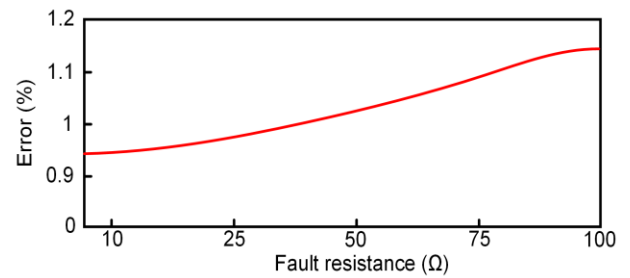

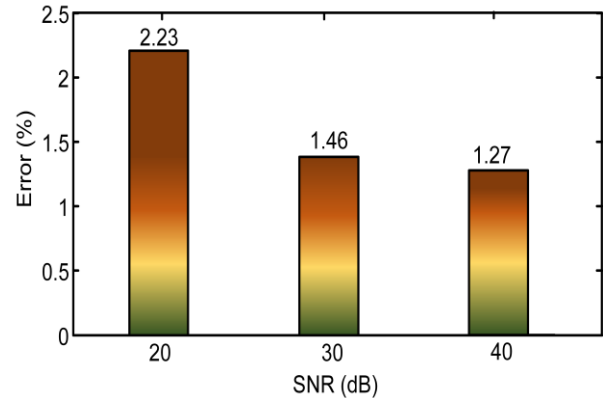**Figure. 5:** Result of proposed algorithm for varying fault resistance

Figure 6: Results of Proposed Algorithm for different noise level

3.5 Influence of line parameters error

To observe the impact of line parameter variation on proposed algorithm, 10% of variation is introduced in the parameters. Table IV displays the effects of the proposed method in terms of the cumulative error estimate of the fault distance along with other current methods[10],[11],[13] and[16] during various ground and phase faults. From Table IV it is observed that the maximum fault distance estimation error provided by the proposed method, unlike other methods, remains less than 1.2 percent even with 10 percent errors in line parameters. Whereas, other existing methods has the error more than 5 %.

Table 4 Performance Evaluation of the Proposed Method in case of Errors in Line Parameters

Algorithm	Fault distance estimation error (%)
Proposed	1.17
[10]	9.41
[11]	11.39
[13]	11.56
[16]	12.83

4. COMPARATIVE EVALUATION

A comparative analysis of proposed with reference to another existing methods algorithm is depicted in Table V. From the Table V, one can conclude that the proposed algorithm is reliable and does not require any synchronized measurement. In addition, the proposed algorithm is independent of line parameters and also it is immune to high fault resistance. Further, the results shown in Table V for SNR of 20 dB proves the superiority of proposed fault location algorithm compared to other existing methods.

Table 5 Comparative Evaluation of the Proposed Method with other Methods

Criterion	Proposed Method	[10]	[11]	[13]	[16]
Requirement of synchronized measurement	X	✓	✓	✓	✓
Independent of line parameters	✓	X	X	X	X
Fault distance estimation error for SNR 20 dB	2.23	6.81	7.43	5.67	6.38

5. CONCLUSION

Due to different attenuation experienced by aerial-mode and earth-mode component of travelling wave, the wave velocity of earth mode increases with the propagation distance. Authors have proposed a traveling wave based fault location algorithm for two-terminal transmission line which utilizes the arrival time difference of zero-mode and aerial-mode component of traveling wave. WTMM is used to detect the time of waves. The proposed algorithm neither needs synchronized measurement nor line parameters, which makes the implementation of scheme economically cheaper. The effectiveness of proposed algorithm to estimate the fault distance is verified by simulating diverse fault cases. The result reported in paper clearly demonstrates the effectiveness of the algorithm to accurately estimate the fault distance.

REFERENCES

[1] Girgis, D. Hart, and W. Peterson. **A new fault location technique for two-and three-terminal lines**. *IEEE Trans. Power Del.*, Vol. 7, no. 1, pp. 98–107, Jan. 1992.

[2] J. Izykowski, E. Rosolowski, P. Balcerek, M. Fulczyk, and M. Saha. **Accurate noniterative fault location algorithm utilizing two-end unsynchronized measurements.** *IEEE Trans. Power Del.*, Vol. 25, no. 1, pp. 72–80, Jan. 2010.

[3] J. Izykowski, E. Rosolowski, P. Balcerek, M. Fulczyk, and M. Saha. **Accurate noniterative fault location algorithm utilizing two-end unsynchronized measurements**. *IEEE Trans. Power Del.*, Vol. 25, no. 1, pp. 72–80, Jan. 2010.

[4] C.-S. Yu. **An unsynchronized measurements correction method for two-terminal fault-location problems.** *IEEE Trans. Power Del.*, Vol. 25, no. 3, pp. 1325–1333, Jul. 2010.

[5] J. Izykowski, R. Molag, E. Rosolowski, and M. Saha. **Accurate location of faults on power transmission lines with use of two-end unsynchronized measurements.** *IEEE Trans. Power Del.*, Vol. 21, no. 2, pp. 627–633, Apr. 2006.

[6] M. M. Saha, J. Izykowski, E. Rosolowski, and R. Molag. **ATP-EMTP investigation of a new algorithm for locating faults on power transmission lines with use of two-end unsynchronized measurements**. presented at the *Int. Conf. Power Syst. Transients*, Lyon, France, Jun. 2007.

[7] M. M. Saha, J. Izykowski, and E. Rosolowski**. Fault Location on Power Networks** (ser. Power Systems). London, U.K.: Springer, 2010.

[8] V. K. Gaur and B. Bhalja. **A new faulty section identification and fault localization technique for three-terminal transmission line.** *Int. J. Electr. Power Ener. Syst*, Vol. 93, pp. 216-227, 2017.

[9] V. K. Gaur and B. Bhalja. **New fault detection and localisation technique for double-circuit three-terminal transmission line**. *IET Gen., Trans. & Distri.*, Vol. 12, no. 8, pp. 1687-1696, 2018.

[10] Spoor, D.; Zhu, J.G. **Improved single-ended traveling-wave fault-location algorithm based on experience with conventional substation transducers**. *IEEE Trans. Power Deliv*. **2006**, 21, 1714–1720. https://doi.org/10.1109/TPWRD.2006.878091

[11] Chen, Y.; Liu, D.; Xu, B.Y. **TravellingWave Single End Fault Location Method based on Network Information**. Prz. Elektrotech. 2012, 88, 205–209.

[12] Lin, S.; He, Z.Y.; Li, X.P.; Qian, Q.Q. **Travelling wave time-frequency characteristic-based fault location method for transmission lines.** *IET Gener. Transm. Distrib.* 2012, 6, 764–772.

[13] Hamidi, R.J.; Livani, H. **Traveling-Wave-Based Fault-Location Algorithm for Hybrid Multiterminal Circuits**. *IEEE Trans. Power Deliv*. 2017, 32, 135–144.

[14] Shaik, A.G.; Pulipaka, R.R.V. **A new wavelet based fault detection, classification and location in transmission lines.** *Int. J. Electr. Power Energy Syst.* 2015, 64, 35–40.

[15] Chen, X.; Yin, X.; Deng, S. **A novel method for SLG fault location in power distribution system using time lag of travelling wave components.** *IEEE Trans. Electr. Electron. Eng.* 2017, 12, 45–54.

[16] Jia, H. **An Improved Traveling-Wave-Based Fault Location Method with Compensating the Dispersion**

Effect of Traveling Wave in Wavelet Domain. *Math. Probl. Eng*. 2017, 2017, 1019591.

[17] Lopes, F.V.; Silva, K.M.; Costa, F.B.; Neves, W.L.A.; Fernandes. *D.* **Real-time traveling-wave-based fault location using two-terminal unsynchronized data**. *IEEE Trans. Power Deliv*. 2015, 30, 1067–1076.

[18] B. J. Cory and P. Gale. **Satellites for power system applications**. *Power Eng. J.*, Vol. 7, no. 5, pp. 201–207, 1993.

[19] M. M. Saha, J. Izykowski, and E. Rosolowski. **Fault Location on Power Networks**, ser. Power Systems. London, U.K.: Springer, 2010, Ed.

[20] H. Lee and A. Mousa. **GPS travelling wave fault locator systems: Investigation into the anomalous measurements related to lightning strikes**. *IEEE Trans. Power Del*., Vol. 11, no. 3, pp. 1214–1223, Jul. 1996.

[21] F. Costa, B. Souza, and N. Brito. **Real-time detection of fault-induced transients in transmission lines**. *IET Elect. Lett.*, Vol. 46, no. 11, May 2010.

[22] F. B. Costa, B. A. Souza, N. S. D. Brito, J. A. C. B. Silva, and W. C. Santos. **Real-time detection of transients induced by high-impedance faults based on the boundary wavelet transform**. *IEEE Trans. on Industry Applications,* Vol. 51, pp. 5312–5323, Nov 2015.

[23] X. Dong, S. Luo, S. Shi, B. Wang, S. Wang, L. Ren, and F. Xu. **Implementation and application of practical traveling-wave-based directional protection in uhv transmission lines**. *IEEE Trans. on Power Delivery*, Vol. 31, pp. 294–302, Feb 2016.

[24] M. Aqib et al. **Agarwood Oil Quality Classification using Support Vector Classifier and Grid Search Cross Validation Hyperparameter Tuning.** *Int. J. Emerg. Trends Eng. Res.*, Vol. 8, no. 6, pp. 6–11, 2020. https://doi.org/10.30534/ijeter/2020/55862020

[25] N. V. S. P. Kumar, J. K. R. Sastry and K. R. S. Rao. **Mining negative frequent regular itemsets from data streams**. *International Journal of Emerging Trends in Engineering Research,* **Vol.** 7, No. 8, pp. 85-98, 2019 https://doi.org/10.30534/ijeter/2019/0278201